Arch. Metall. Mater. **64** (2019), 4, 1309-1314

DOI: 10.24425/amm.2019.130095

A. MAZUREK*#, M. TRZASKA*

STRUCTURE AND PROPERTIES OF Ni/DIAMOND NANOCRYSTALLINE COATINGS

This paper presents the results of research of Ni/diamond composite coatings produced by electrochemical reduction method. Research was focused on composite coatings with nickel matrix and diamond as a disperse phase and for comparison purposes on nanocrystalline nickel coatings. Ni/diamond composite coatings were produced in baths with different content of nanodiamond powder. The structures of the dispersed phase and the composite coatings were analysed by using X-ray diffraction, scanning electron microscopy and light microscopy. Measurements of selected properties of the coatings were performed, including roughness, microhardness, adhesion and abrasive wear resistance. The research results indicate that the produced coatings have a compact structure and good adherence to steel substrate. Moreover, nanocrystalline Ni/diamond composite coatings exhibit greater hardness and reduced abrasive wear resistance compared to nanocrystalline nickel coatings.

Keywords: diamond, nickel/diamond, composite coatings

1. Introduction

Electrocrystallization is one of the main methods of producing coatings that increases the resistance of products to mechanical damage and corrosion. This method also enables producing coatings of composite materials with metal matrix and dispersed phase made from different materials. Using electrocrystallization to produce composite coatings involves the simultaneous deposition of metal incorporating a dispersed phase. Depending on purpose of coatings, their properties can be designed and modified by using different matrix and disperse phase materials together with suitable selection of their particle sizes and the content of dispersed phase in composite material. The incorporation of dispersed phases into metal coatings can be beneficial to their mechanical properties [1-3], corrosion resistance [4-6] and antibacterial characteristics [7].

The studies presented in this paper result as a continuation of the authors previous research [6,8] revealing possibilities of producing composite coatings with nickel matrix and diamond powder as dispersed phase. The coatings were deposited on a steel substrate by electrochemical reduction method using a bath of the Watts type. In authors earlier research the diamond powder manufactured by JSC SINTA was used to form the suitable bath. It has been shown previously that the hard disperse phase incorporated into the nickel matrix brought favorable features of the deposited composite coatings.

In the current research the diamond powder manufactured by Nanostructured&Amorphous Materials Inc. with content of 2.5-10 g/dm^3 in the bath was used. The performed research is aimed on determination of influences of diamond powder concentrations in the bath on quantities of incorporated diamond in the nickel matrix and also on mechanical features of the produced coatings.

2. Research methodology

Nickel (Ni) and Ni/diamond composite (Ni/d) coatings were produced on a carbon steel (S235JR) surface using electrochemical reduction approach. The coatings were produced in a modified Watts bath with composition presented in Table 1. The influence of organic additives prevented the formation of material stresses and ensured the fragmentation of the structure of the layers to nanometric size [9].

TABLE 1

Chemical composition of baths

Coating	The content of diamond powder in bath [g/dm^3]	Chemical composition of baths
Ni	—	nickel (II) sulfate (VI), boric acid, nickel (II) chloride saccharin sodium lauryl sulfate
Ni/diamond (2.5)	2.5	
Ni/diamond (5)	5	
Ni/diamond (7.5)	7.5	
Ni/diamond (10)	10	

* ŁUKASIEWICZ RESEARCH NETWORK – INSTITUTE OF PRECISION MECHANICS, 3 DUCHNICKA STR., 01-796 WARSZAWA, POLAND

Corresponding author: anna.mazurek@imp.edu.pl

The Ni/diamond composite coatings were produced in baths with varying diamond powder content: 2.5, 5.0, 7.5 and 10 g/dm^3. The deposition process was performed at a current density of 3 A/dm^2 in the bath at temperature of 45°C. The deposition time was 45 minutes. In order to obtain a homogeneous suspension of the diamond powder in the bath, mechanical strirring with 100 rpm was carried out for 60 minutes before the process. The bath was mechanically stirred during the process to prevent sedimentation (100 rpm).

Transmission electron microscopy (Libra 120, Zeiss) and X-ray diffraction (MiniFlex II, Rigaku) were used to analyse the structure of the disperse phase. The structure of the produced coatings was analysed with X-ray diffractometer (MiniFlex II, Rigaku). The morphology and topography of the surface of the produced coatings were analysed using Zeiss LEO 435VP scanning electron microscope with EDS detector. The development degree of coating surfaces was analysed with Mitutoyo surface roughness tester. A Vickers hardness test was performed to measure the microhardness of the coating material at 98 mN load (HV 0.01), using Buehler T1202 Wilson Hardness tester. A scratch test, using Revetest scratch tester at an increasing load from 1 to 100 N was performed to measure the adhesion between the produced coating and the steel substrate material. The Rockwell spheroconical diamond indenter having 120° cone angle and 200 μm radius spherical tip has been used. The scratch length was 10 mm. The tribological properties of the produced coating material in sliding contact were tested using the ball-on-disc method [10]. The applied test system consisted of a sample and a 5 mm diameter silicon carbide ball pressed against the sample with a force of 7.35 N. In the test, the sample was put in rotary motion (at 2rps), which led to the formation of a wear track with a diameter of 4 mm. The total distance performed during the test was 6.28 m (500 rotations). Dry sliding friction tests were conducted at room temperature.

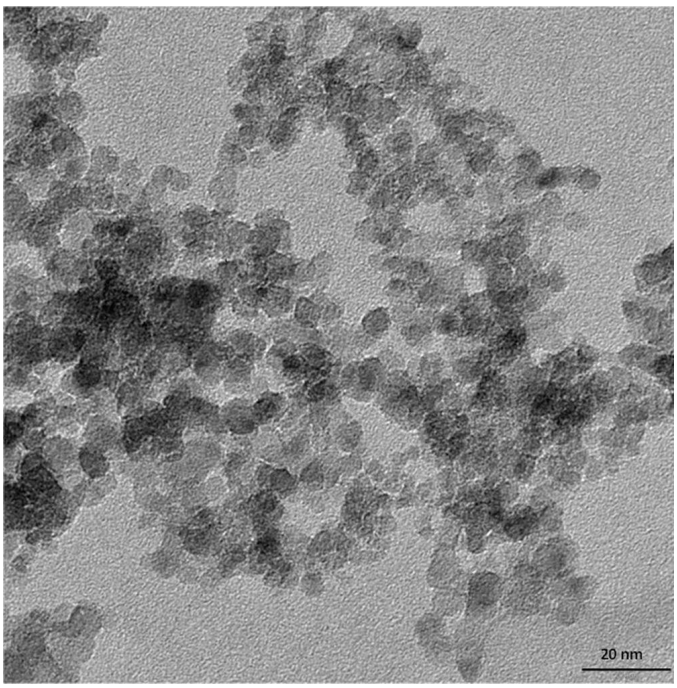

Fig. 1. TEM image of the diamond nanoparticles

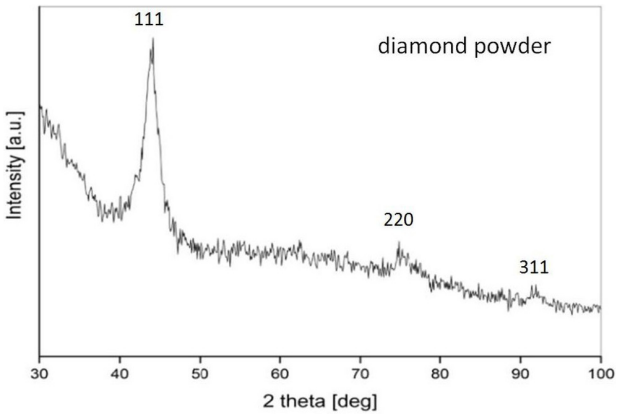

Fig. 2. X-ray diffraction patterns of diamond powder

3. Results

The image of the particles of the diamond powder registered using transmission electron microscopy (TEM) is shown in Figure 1.

The diamond powder particles exhibited a similar shape of sizes less than 10 nm. The results of XRD analysis of the diamond powder are presented in Figure 2. Broadened diffraction reflections confirm the nanometric dimensions of the particles.

Figure 3 shows the results of XRD analysis of the structure of the nickel and composite coatings.

The obtained diffraction patterns prove the crystalline structure of the tested coating materials. The increased reflection width on the diffraction patterns indicates the nanocrystalline structure of both the nickel and the composite coatings.

The significant variation in the intensity of diffraction reflexes on particular diffraction patterns indicates that the coating material is strongly texturized. For the nickel layers, the predominant direction of the nickel crystal growth is <200>. For composite coatings produced in baths with dispersed diamond phases, the predominant direction of the nickel crystal growth is <111>. As a result of the change in the privileged direction of the growth of nickel crystals, the intensity of individual reflexes changes. In the X-ray diffraction pattern of the composite coating, the reflex <220>, characteristic of a diamond (Fig. 2) was observed. The dispersed phase incorporated into the nickel matrix also influences the morphology and topography of composite coatings formed by electrocrystallization method. In the initial stage of the deposition, the metal atoms reproduce the structure of the substrate material. As the coating grows, the nickel-like structure is formed. The mechanism of the formation of composite coatings consists in the simultaneous deposition of the matrix metal and the incorporation of the dispersed phase into the matrix. The images of the surface topography of the produced nickel and composite coatings with different concentration of the dispersed phase are shown in Figure 4.

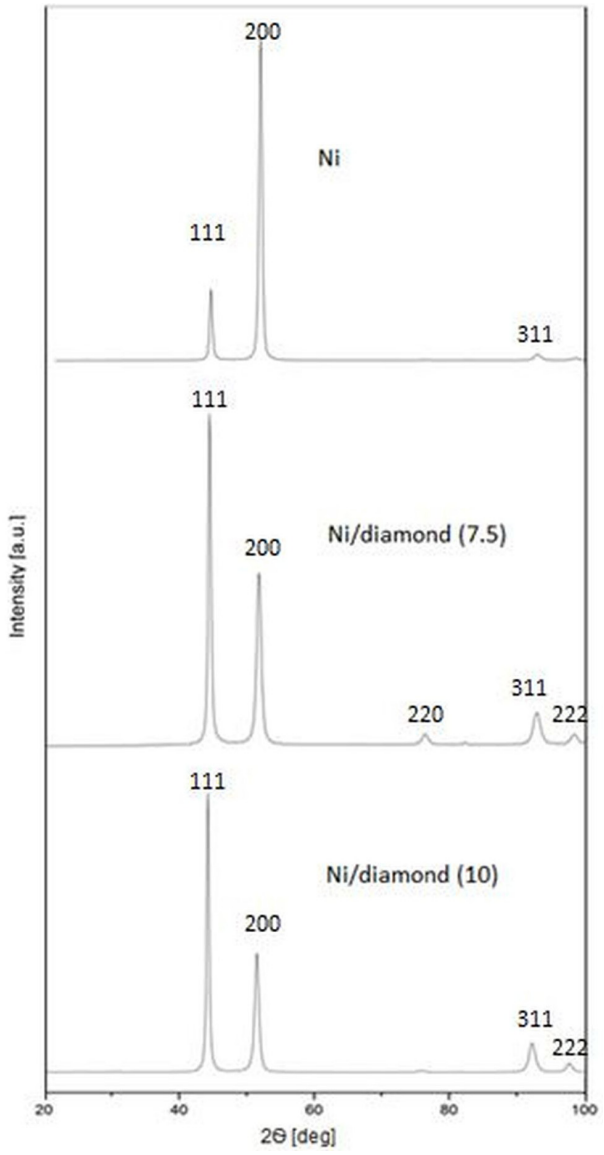

Fig. 3. X-ray diffraction patterns of Ni and composite coatings

On the surface of the Ni/diamond composite coatings, some dispersed phase agglomerates are present that are not entirely covered with the nickel matrix material. The chemical composition of the composite coatings produced in baths of varying content of diamond powder which were analysed in the middle area of the sample using scanning electron microscope with EDS detector is shown in Table 2.

TABLE 2

The content of elements in composite coatings

Composite coating	The content of diamond powder in bath [g/dm^3]	The content of elements in composite coatings [% at.]	
		Ni	C
Ni/diamond (2.5)	2.5	77.9	22.1
Ni/diamond (5)	5	76.4	23.6
Ni/diamond (7.5)	7.5	56.1	43.8
Ni/diamond (10)	10	76.6	23.4

The image of the carbon distribution in the composite layers in which agglomerates of incorporated carbon particles are visible is shown in Figure 5.

Increasing the diamond powder content in the bath from 2.5 to 7.5 g/dm^3 results in an increase in the amount of the diamond dispersed phase incorporated into the composite coating material. However further increase of the diamond powder content in the bath to 10g/dm^3 results in a decrease of the amount of the diamond dispersed phase incorporated into the composite coating material produced with the same parameters of the coating deposition process. The research results indicate that there is a maximum diamond powder concentration in the bath beyond which the amount of incorporated diamond does not increase (at constant process parameters). This relationship attests the data given in [11-13]. Along with the increase in the content of the dispersion phase in the bath, the particles show a greater tendency

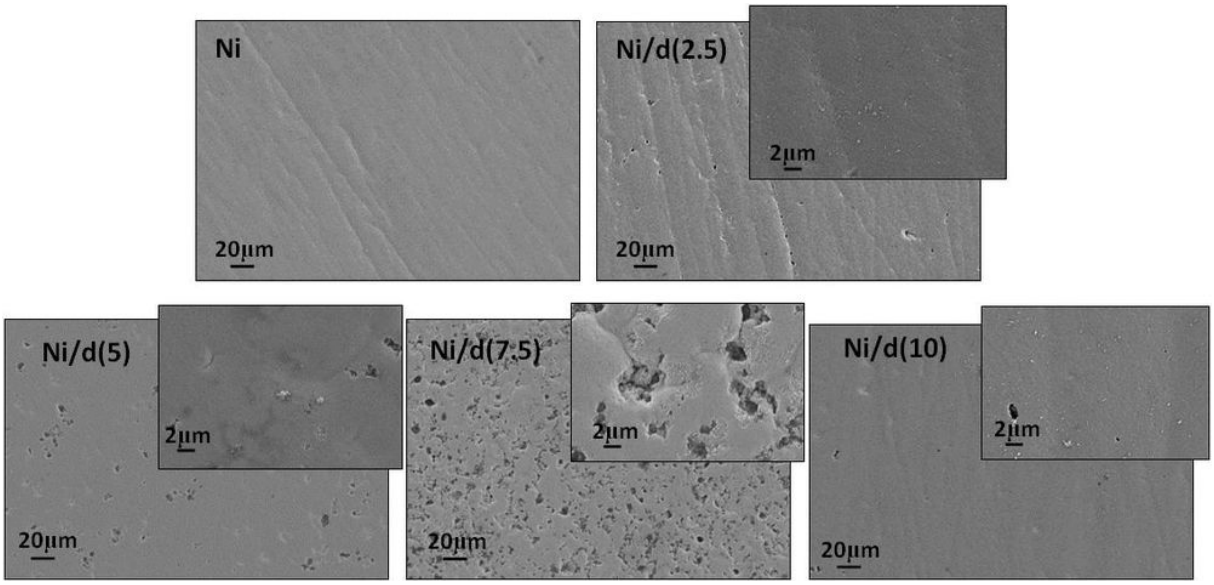

Fig. 4. SEM images of surface topography of produced coatings: a) Ni, b) Ni/diamond 2.5 g/dm^3, c) Ni/diamond 5 g/dm^3, d) Ni/diamond 7.5 g/dm^3, e) Ni/diamond 10 g/dm^3

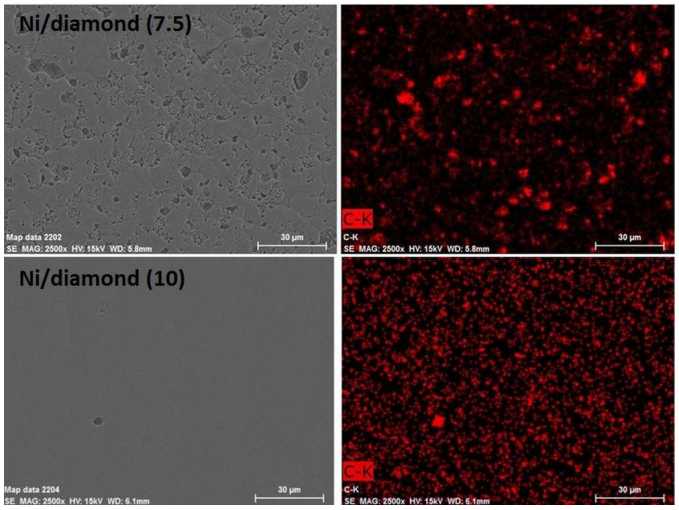

Fig. 5. Distribution of the carbon in composite coatings

to agglomerate. Co-deposition of agglomerates is difficult due to the blocking effect [11]. In addition, the greater amount of dispersed phase in the bath (10g/dm^3) with stirring during the deposition process of the composite coating removes weakly anchored agglomerates from the surface.

The microstructures of the nickel and composite coatings in cross sections perpendicular to the coating surfaces are shown in Figure 6.

Each produced nickel and composite coatings are characterized by compact structure and uniform thickness (20 μm) over the entire substrate surfaces. In the composite coatings, diamond powder agglomerates, quite uniformly distributed across the volume of the material, are present. The amount of diamond embedded in composite coatings affects the degree of surface development. The results of the measurement of the R_a roughness parameter of the substrate and the produced coatings are shown in Table 3.

TABLE 3

Roughness of the substrate and the produced coatings

Material	Ra [μm]	
	Steel	Coating
Ni	0.058	0.076
Ni/diamond (2.5)	0.073	0.105
Ni/diamond (5)	0.058	0.085
Ni/diamond (7.5)	0.084	0.245
Ni/diamond (10)	0.113	0.138

In nickel coatings, the difference in roughness of the coating compared to that of the substrate surface is negligible. The Ni/diamond composite coating with the greatest content of incorporated diamond dispersed phase is characterized by the greatest roughness.

The quality of the surface coatings in practical applications is also determined by their adherence to the substrate. Results of the scratch tests performed to determine the adherence of the produced Ni and Ni/diamond composite coatings to the substrate are shown in Figure 7.

In a scratch test, an indenter pressed with a progressive load against the tested surface, caused elastic and plastic deformation of the coatings material. A scratch with elevated edges was formed on the coating surface. Based on studies carried out, there were not any delaminations of the coatings from the substrate material. Only small cohesive cracks inside the area of the scratch were observed as a results of the deformation of the coating material by the intender. The L_{C1} critical loads at which failure of the coating is initiated in the form of cohesive cracks are summarized in Table 4. The performed studies show that all layers have a good connection to the substrate material (Fig. 7).

The incorporation of diamond nanoparticles in the nickel matrix impacts the microhardness of the coating material. A Vickers test at a load of 98 mN (HV0.01) was conducted to measure the microhardness of the substrate material and produced coat-

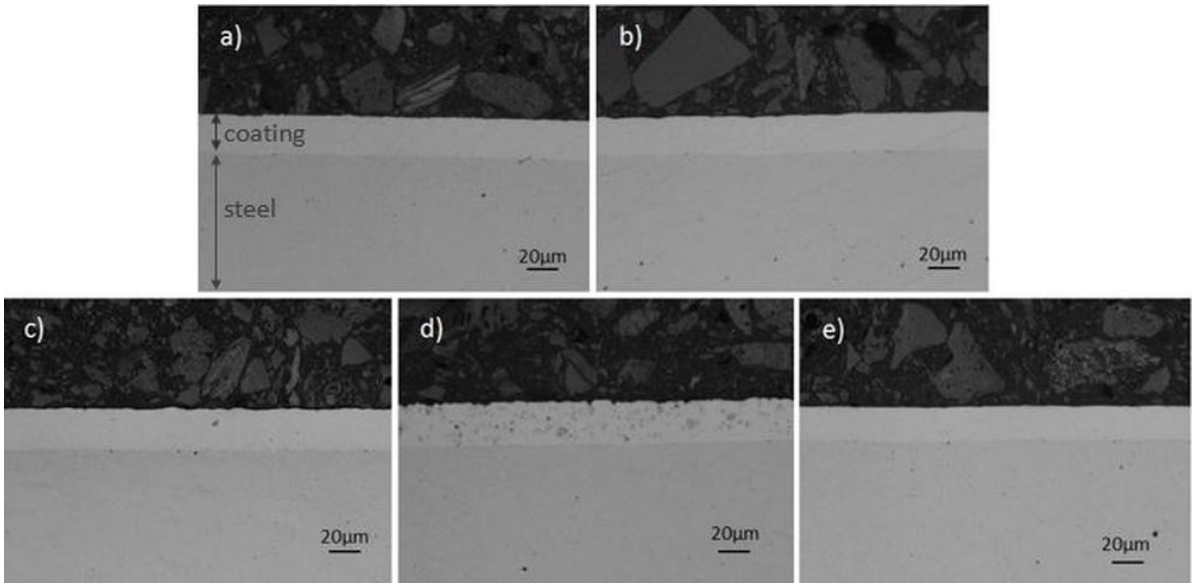

Fig. 6. Microstructures in the cross-sections of Ni (a) and Ni/diamond coatings: b) Ni/diamond 2.5 g/dm^3, c) Ni/diamond 5 g/dm^3, d) Ni/diamond 7.5 g/dm^3, e) Ni/diamond 10 g/dm^3

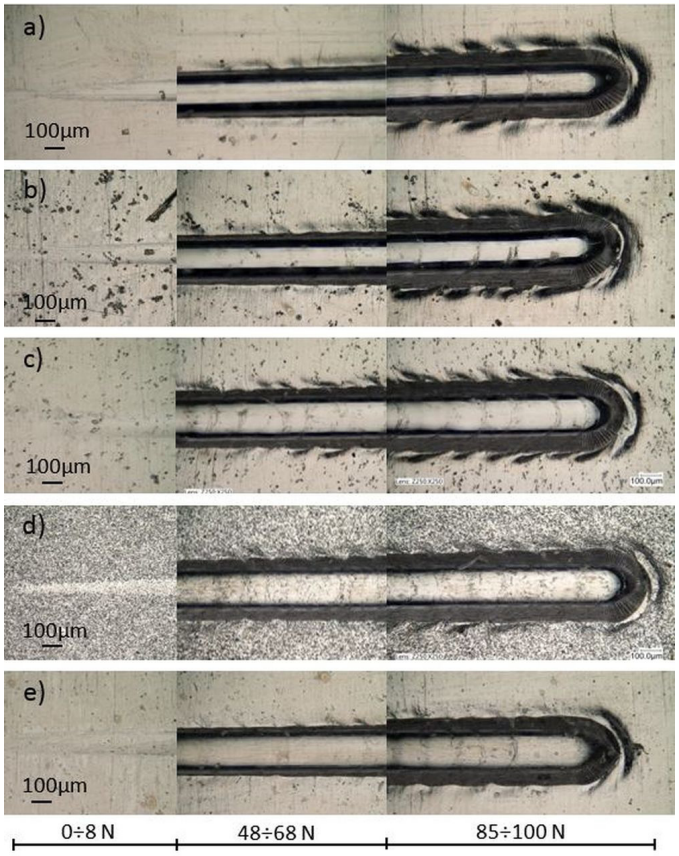

Fig. 7. Images of scratches on the coatings after scratch tests: a) Ni, b) Ni/diamond 2.5 g/dm^3, c) Ni/diamond 5 g/dm^3, d) Ni/diamond 7.5 g/dm^3, e) Ni/diamond 10 g/dm^3

TABLE 4

Cohesive critical load

Coatings	Cohesive critical load L_{C1} [N]
Ni	95.1
Ni/diamond (2.5)	66.5
Ni/diamond (5)	56.2
Ni/diamond (7.5)	53.4
Ni/diamond (10)	90.9

ings on cross-sections perpendicular to the coating surface. The results of the tests are shown in Fig. 8.

As expected, the incorporation of the nanoparticles of the hard diamond phase into the nanocrystalline nickel matrix increased the hardness of the coating material. The increase in

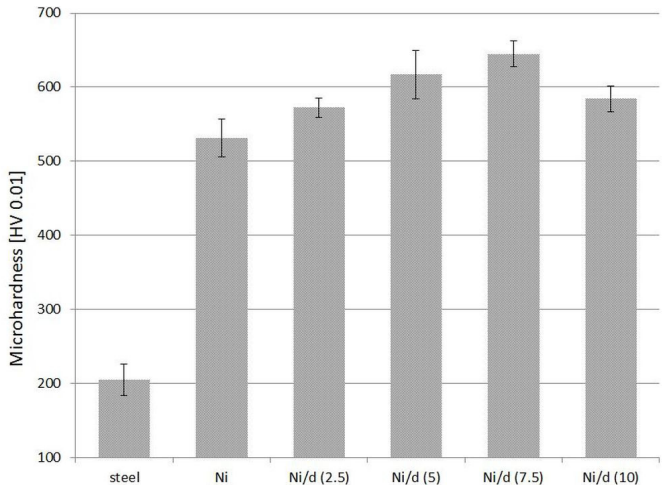

Fig. 8. Microhardness of the substrate material and produced coatings

hardness may be associated with two strengthening mechanisms, which are observed in composite materials: strengthening of grain boundaries and dispersion strengthening [14].

Microhardness tests show that the amount of a dispersed phase contained in a composite material influences the hardness of the material. The greatest hardness is achieved in coatings deposited in a bath with the diamond concentration of 7.5 g/dm^3.

The type of material, its structure, hardness and degree of surface development influence tribological properties of the coating materials. The tribological properties of the produced coatings were tested in dry sliding contact using the ball-on-disc method [10]. There were no wear of the abrasive ball. As the wear criterion the abrasion depth was taken. The results of abrasive wear tests of substrate material and produced coatings are shown in Figures 9 and 10.

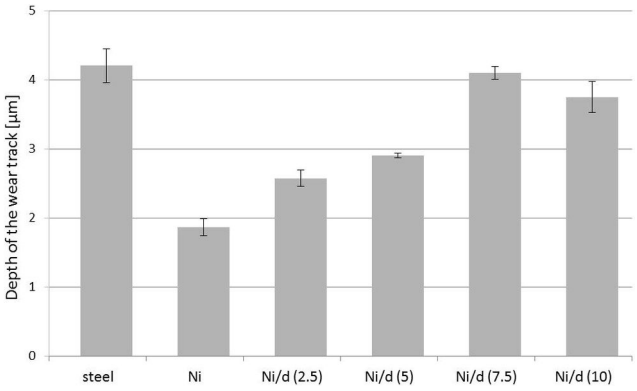

Fig. 9. Abrasive wear of Ni and Ni/diamond coatings

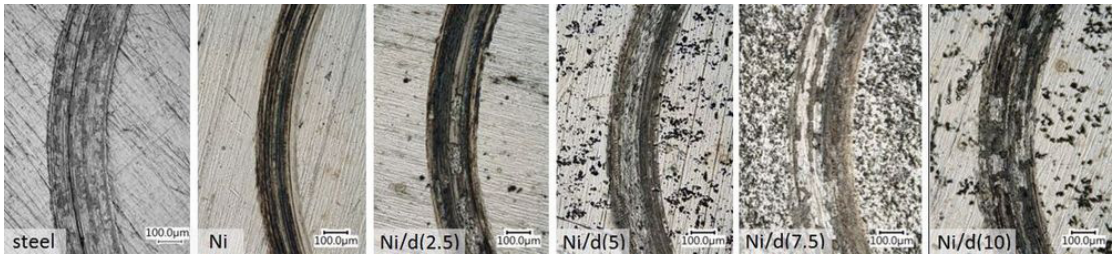

Fig. 10. Images of abrasion traces on the coating surfaces after ball-on-disc studies

Composite coatings Ni/diamond are characterized by a lower wear resistance compared to nickel coating. During the wear test, the hard particles of the diamond dispersed phase pulled out from the coating act as abrasive in the friction zone. It results in increased wear of the coating material [11].

4. Conclusions

Electrocrystallization can be effectively used to produce nanocrystalline Ni/diamond composite coatings with different content of diamond dispersed phases. Composite coatings produced using this method are characterized by a compact structure, uniform thickness over the entire surface and good adherence to the substrate material. The incorporation of diamond particles in the nanocrystalline nickel matrix increases the degree of development of the coating surface. Nanocrystalline Ni/diamond composite coatings with a diamond (22-43% at. of C) exhibit greater hardness and reduced abrasive wear resistance compared to nanocrystalline nickel coatings.

REFERENCES

[1] V.V.N. Reddy, B. Ramamoorthy, P. Kesavan Nair, Wear **239**, 111-116 (2000).

[2] K.-H. Hou, H.-T. Wang, H.-H. Sheu, M.-D. Ger, Appl. Surf. Sci. **308**, 372-379 (2014).

[3] Z. Karaguiozova, J. Kaleicheva, V. Mishev, G. Nikolcheva, Tribol. Int. **39**, 444-451 (2017).

[4] H. Mazaheri, S.R. Allahkaram, Appl. Surf. Sci. **258**, 4574-4580 (2012).

[5] M. Sajjadnejad, H. Omidvar, M. Javanbakht, A. Mozafari, J. Alloy Compd. **704**, 809-817 (2017).

[6] M. Trzaska, A. Mazurek, Corrosion Protection **11**, 404-406 (2015).

[7] Y. Reyes-Vidal, R. Suarez-Rojas, C. Ruiz, J. Torres, S. Talu, A. Mendez, G. Trejo, Appl. Surf. Sci. **342**, 34-41 (2015).

[8] M. Trzaska, A. Mazurek, Composite Theory and Practice **1**, 37-41 (2016).

[9] N.P. Wasekar, P. Haridoss, S.K. Seshadri, G. Sundararajan, Surf. Coat. Tech. **291**, 130-140 (2016).

[10] A. Kondej, Surface Engineering **1**, 76-79 (2017).

[11] M. Pushpavanam, H. Manikandan, K. Ramanathan, Surf. Coat. Tech. **201**, 6372-6379 (2007).

[12] M.K. Das, R. Li, J. Qin, X. Zhang, K. Das, A. Thueploy, S. Limpanart, Y. Boonyongmaneerat, M. Ma, R. Liu. Surf. Coat. Tech. **301**, 337-343 (2017).

[13] H. Ogihara, M. Safuan, T. Saji, Surf. Coat. Tech **212**, 180-184 (2012).

[14] F. Hou, W. Wang, H. Guo, Appl. Surf. Sci. **252**, 3812-3817 (2006).